

# InFOC $\mu$ S hard X-ray imaging telescope

J. Tueller · H. A. Krimm · T. Okajima ·  
S. D. Barthelmy · S. M. Owens · P. J. Serlemitsos ·  
Y. Soong · K.-W. Chan · Y. Ogasaka · R. Shibata ·  
K. Tamura · A. Furuzawa · Y. Tawara · H. Kunieda ·  
K. Yamashita

Received: 15 January 2006 / Accepted: 14 February 2006  
© Springer Science + Business Media B.V. 2006

**Abstract** InFOC $\mu$ S is a new generation balloon-borne hard X-ray telescope with focusing optics and spectroscopy. We had a successful 22.5-hour flight from Fort Sumner, NM on September 16,17, 2004. In this paper, we present the performance of the hard X-ray telescope, which consists of a depth-graded platinum/carbon multilayer mirror and a CdZnTe detector. The telescope has an effective area of 49 cm<sup>2</sup> at 30 keV, an angular resolution of 2.4 arcmin (HPD), and a field of view of 11 arcmin (FWHM) depending on energies. The CdZnTe detector is configured with a 12 × 12 segmented array of detector pixels. The pixels are 2 mm square, and are placed on 2.1 mm centers. An averaged energy resolution is 4.4 keV at 60 keV and its standard deviation is 0.36 keV over 128 pixels. The detector is surrounded by a 3-cm thick CsI anti coincidence shield to reduce background from particles and photons not incident along the mirror focal direction. The inflight background is  $2.9 \times 10^{-4}$  cts cm<sup>-2</sup> sec<sup>-1</sup> keV<sup>-1</sup> in the 20–50 keV band.

**Keywords** Hard X-rays · Multilayer mirror · CdZnTe pixellated detector · Balloon experiments · Background

## 1. Introduction

The International Focusing Optics Collaboration for  $\mu$ Crab Sensitivity (InFOC $\mu$ S) is a balloon-borne experiment with an X-ray imaging telescope in the hard X-ray band above 20 keV, where space-borne hard X-ray telescopes have not been available so far. Hard X-ray imaging observations, however, are very important to investigate strongly obscured objects,

---

J. Tueller · H. A. Krimm · T. Okajima (✉) · S. D. Barthelmy · S. M. Owens · P. J. Serlemitsos ·  
Y. Soong · K.-W. Chan  
NASA Goddard Space Flight Center, Greenbelt, MD 20771, USA  
e-mail: okajima@milkyway.gsfc.nasa.gov

Y. Ogasaka · R. Shibata · K. Tamura · A. Furuzawa · Y. Tawara · H. Kunieda · K. Yamashita  
Nagoya University, Furo-cho, Chikusa, Nagoya, Aichi, 464-8602, Japan

study nuclear  $\gamma$ -ray lines from SNR, resolve hard X-ray emission from clusters of galaxies, understand acceleration mechanisms, discover new objects, and so on.

InFOC $\mu$ S intends to have multiple hard X-ray telescopes covering broad energy band from 20 keV up to 80 keV. The lower energy limit of 20 keV comes from atmospheric absorption, and the higher energy limit from the K absorption edge of a mirror material (platinum). In previous five years, InFOC $\mu$ S flew four times including a test flight with the CZT detector only in 2000. Developments and improvements of the mirror and detector have been continuously done. In the most recent flight from Fort Sumner, NM on September 16, 2004, we had a successful 22.5-hour flight. We observed X-ray binaries, a galactic black hole candidate, a cluster of galaxies, and a Seyfert galaxy (Ogasaka et al., 2005). In this paper, we present performance of the multilayer mirror and CZT detector system for the 2004 flight. The inflight detector background and sensitivity are also presented.

## 2. InFOC $\mu$ S instruments overview

The InFOC $\mu$ S hard X-ray telescope consists of a depth-graded platinum/carbon multilayer mirror and a CdZnTe detector. The hard X-ray mirror is made of conical thin-foil mirrors (170  $\mu$ m thick) which is similar to the *Suzaku* X-ray telescope (Kunieda et al., 2001), but with Pt/C multilayer mirror on the reflector surface and the longer focal length of 8 m. Its diameter is 40 cm and 255 mirror shells are nested in the mirror housing (Figure 1). The pixellated CdZnTe detector is configured with a  $12 \times 12$  segmented array of detector pixels. The detector and pixel size are 1 inch and  $2 \times 2$  mm<sup>2</sup>, respectively. The detector is placed on the top of an aluminum cube with an ASIC (Figure 2). It is surrounded by a 3-cm thick CsI with 11 PMTs. They make an active shield utilizing anticoincidence of signals from the PMT and detector to reduce non X-ray background. The detector also has a tagged source system with <sup>241</sup>Am to monitor the energy gain of the detector during the flight.

Figure 3 shows the InFOC $\mu$ S gondola. The mirror mounted on the left hand side of the truss structure. The detector is placed inside the pressure vessel on the other end of the truss. The gondola is an elevation-over-azimuth system. The truss is coupled to the center gondola platform at its center of gravity, and is attached into elevation direction by long-threaded screw driven by a DC motor mounted on the gondola platform. The whole gondola system is driven into azimuthal direction by a reaction wheel mounted on the gondola platform

**Fig. 1** Pt/C depth-graded multilayer hard X-ray mirror.



**Fig. 2** Pixallated CdZnTe hard X-ray detector.



**Fig. 3** InFOC $\mu$ S flight gondola.



and also by a decoupler motor placed between the balloon and payload. Attitude sensors such as three-axis rate gyros, magnetometers, level sensors and differential GPS sensors are mounted on the gondola platform to determine its attitude. An elevation axis resolver determines relative elevation angle of the optical truss with respect to the gondola platform. Independent and absolute attitude sensors are mounted on the optical truss; a boresight star camera and differential GPS sensor. The specification of the InFOC $\mu$ S instruments are summarized in Table 1.

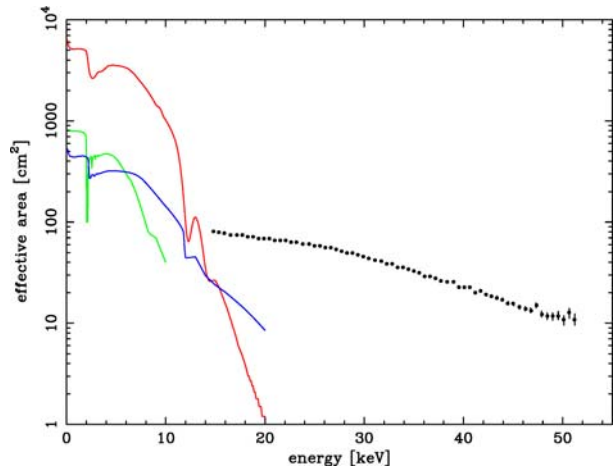
### 3. Depth-graded multilayer mirror

The InFOC $\mu$ S multilayer mirror was developed by Nagoya University and NASA/GSFC. Pt/C multilayer mirrors were deposited by a DC magnetron sputtering system. In order to control quality of mirrors during the production, their reflectivity for about 20% of all the mirrors was quickly measured using monochromatic W-L $\alpha$  X-ray (8.4 keV). Measurement was performed by  $\theta - 2\theta$  angular scanning. Some of mirrors were also measured with continuum X-rays up to 50 keV at a fixed incident angle. For example, we obtained reflectivity of more than 50% up to 35 keV at the incident angle of 0.187 deg. Quality of X-ray mirrors can be

**Table 1** Summary of InFOC $\mu$ S instruments for the 2004 flight

Pt/C multilayer mirror		CdZnTe detector assembly	
Energy	<50 keV	Detector size	1 × 1 inch
Diameter/focal length	40 cm/8 m	Pixel array	12 × 12 (128 active pixels)
Optics	Conical Appr. of Wolter I	Pixel spacing	2.1 mm
Incident angle	0.105–0.356 deg.	Pixel size/thickness	2 × 2 mm <sup>2</sup> /2mm
Number of nesting	255	Operating temperature	27 deg. C
Number of reflectors	2040	Detection efficiency	~100%(<50 keV)
Reflector	Al-backed epoxy replica	Active shield	3-cm thick CsI with PMTs
Reflector radius	59–200 mm	Collimator FOV	10 deg. (FWHM)
Reflector length	100 mm × 2		
Reflector thickness	170 $\mu$ m		
Reflector surface	Pt/C multilayer	Tagged source	<sup>241</sup> Am
Periodic thickness	29–130 Å		(tagged by anti-coincidence)
Number of bi-layers	25–65		
Gondola system			
Dimensions/weight	9m-long × 5m-height/~1600 kg		
Attitude control	Elevation-over-azimuth system+tilt-adjustment straps		
Attitude determination	Star camera, gyroscopes, Magnetometers, Level sensors		

**Fig. 4** Measured effective area of the InFOC $\mu$ S telescope (dots with errors) compared with *Chandra* (green), *XMM-Newton* (red) and *Suzaku* (blue).



also characterized by roughness of mirror surface and interface between layers. The roughness is represented by a Debye-Waller factor. Average roughness of our multilayer sample is  $0.34 \pm 0.05$  nm and gradually increase toward larger radii of the mirror. Once we finished the production of all mirrors, we assemble them into the full hard X-ray mirror (Figure 1).

Pre-flight ground calibration of the hard X-ray mirror was performed at ISAS/JAXA and the synchrotron facility, SPring-8 in Japan. A soft X-ray characteristic, such as effective area, angular resolution, and field of view (FOV), was measured at ISAS with Cu-K $\alpha$  (8 keV) using a NaI scintillation detector and X-ray CCD. Hard X-ray measurement above 10 keV was done at SPring-8 using a position sensitive NaI+CCD detector. Detail of the measurement are described in Shibata et al. (2005). Figure 4 shows a measured on-axis effective area of the InFOC $\mu$ S mirror compared with soft X-ray mirrors (*Chandra*, *XMM-Newton*, and *Suzaku*). The InFOC $\mu$ S mirror has a significant effective area above 10 keV. Measured effective area

**Table 2** Summary of measured effective area and field of view (FOV)

Energy [keV]	Effective area [cm <sup>2</sup> ]	FOV [arcmin]
20	68	12
30	49	11.5
40	23	11
50	11	

**Fig. 5** Vignetting functions of the mirror at various energy bands.

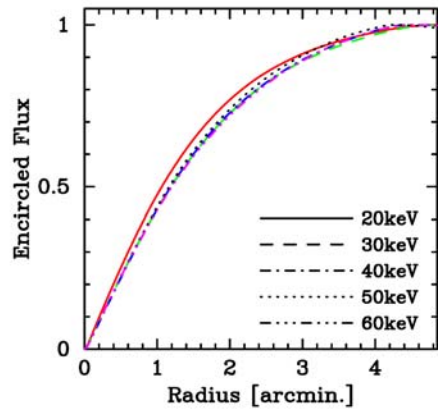
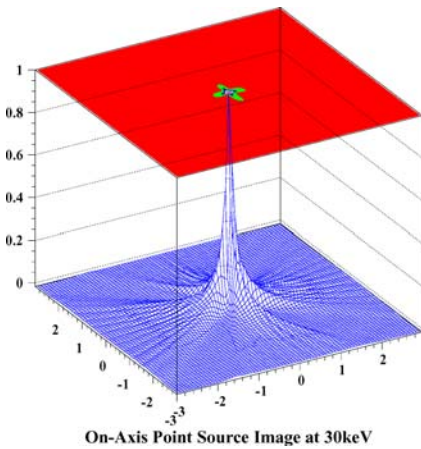
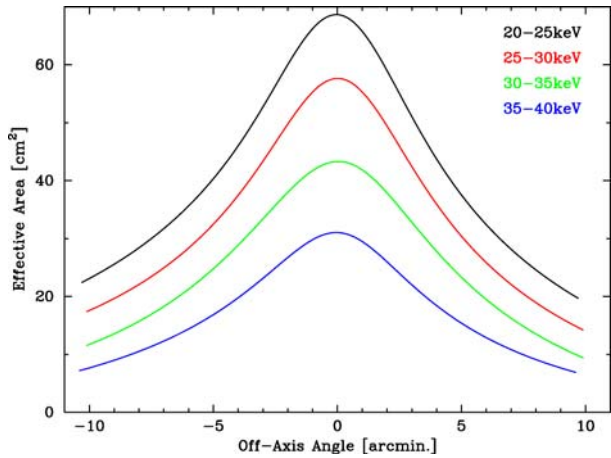


**Fig. 6** 3D image of InFOCμS telescope measured with 30 keV monochromatic X-rays (left). Encircled energy functions of 20–60 keV with 10 keV step (right).

is summarized in Table 2. Figure 5 shows vignetting functions at various energy bands. FOVs defined by FWHM of the vignetting function are also listed in Table 2.

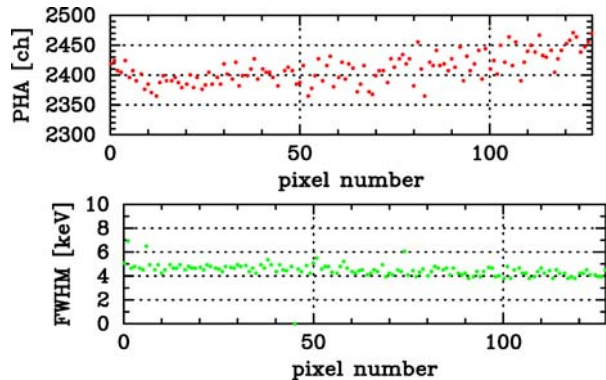
A point spread function (PSF) and encircled energy function (EEF) were evaluated by using monochromatic parallel hard X-ray beam of 20–60 keV with 10 keV step. Figure 6 shows an on-axis image with monochromatic parallel X-ray beam of 30 keV and the EEFs with 20–60 keV. Half power diameter (HPD) of this mirror is 2.1–2.4 arcmin in the above energy band, and it has almost no energy dependence.

#### 4. CdZnTe detector

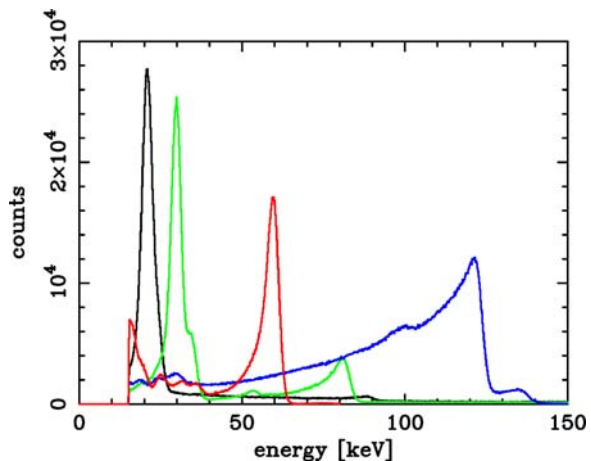
The InFOC $\mu$ S CdZnTe detector was developed by NASA/GSFC. We performed a pre-flight detector calibration in order to characterize the detector performance, such as energy-channel relations of individual pixels, distributions of energy gains and offsets over 128 pixels, and energy resolution. Tagged source spectra were obtained to monitor the energy gain during the flight.

The pre-flight calibration data was taken under the flight conditions. The detector temperature is 27 deg C, which is controlled by a thermal electric cooler. The bias voltage is 200 V. With this configuration, the leakage current is 27 nA. The entire detector was illuminated with radioactive sources,  $^{109}\text{Cd}$ ,  $^{133}\text{Ba}$ ,  $^{241}\text{Am}$ , and  $^{57}\text{Co}$ , to get relations between raw PHA channel and energy for each pixel. The top panel of Figure 7 shows a distribution of PHA channels corresponding to the 60 keV peak of  $^{241}\text{Am}$ . It distributes over 100 channels around 2400 ch for 128 pixels. Using multiple peaks from radioactive sources, we found the conversion (gain and offset) from the PHA channel to energy. We find that the gain is about 0.22 keV/channel and channel-energy relation is linear up to 122 keV ( $^{57}\text{Co}$ ). The FWHM of the 60 keV peak is  $4.4 \pm 0.36$  keV. The bottom panel of Figure 7 shows the distribution of FWHM for the 60 keV peak. Once we convert PHA channel to energy, we can add all pixel spectra together to make a spectrum for the entire detector. Figure 8 shows spectra

**Fig. 7** The top panel shows the distribution of 60 keV peak position ( $^{241}\text{Am}$ ) in PHA channel and the bottom panel FWHM of the 60 keV line (energy resolution).

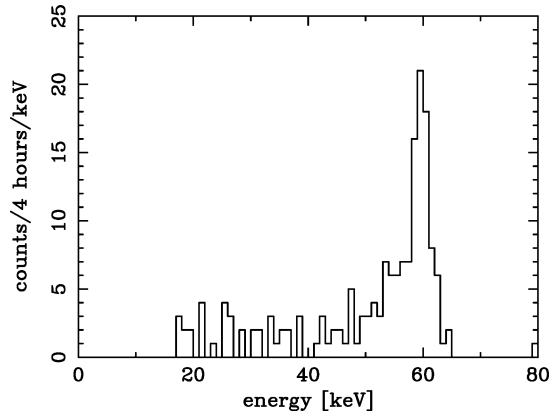


**Fig. 8** Calibration spectra. Peaks from left to right are 22 ( $^{109}\text{Cd}$ ), 30 ( $^{133}\text{Ba}$ ), 60 ( $^{241}\text{Am}$ ), and 122 ( $^{57}\text{Co}$ ) keV, respectively.



**Table 3** Measured energy resolution from the entire detector spectra

Energy [keV]	Resolution (FWHM) [keV]
22 ( $^{109}\text{Cd}$ )	$4.1 \pm 0.047(18.6\%)$
30 ( $^{133}\text{Ba}$ )	$3.8 \pm 0.052(12.7\%)$
60 ( $^{241}\text{Am}$ )	$4.0 \pm 0.059(6.7\%)$

**Fig. 9** An example of tagged source spectrum (four hour accumulation) for pixel #32.

from different radio active sources for the entire detector. One can see large tail associated with peaks, especially for the 122 keV peak of  $^{57}\text{Co}$ . This is due to loss of holes during the travel inside the CZT. Low energy photons are absorbed close to the top surface, while higher energy photons interact inside the detector. Holes have to travel longer paths to be collected. Measured energy resolutions of the entire detector spectra are summarized in Table 3.

We extracted tagged source spectra by collecting only tagged events so that we were able to check not only the channel-energy relation but also the energy resolution during the flight, compared with the ground calibration results. Figure 9 shows spectrum for pixel #32 with four hours accumulation as an example. The count rate of tagged events is 1.3 cts/sec for the entire detector (20–65 keV), so that rate for the 60 keV line is 0.005 cts/sec for one pixel. In the four hour accumulation, we can get 72 cts for the line. The peak position can be determined with 1 keV accuracy. Extracting the tagged source spectra every 30 minutes to check the gain stability, we found that the peak position was stable within  $\pm 2$  ch, which corresponds to about 0.44 keV. And the energy resolution is consistent with that in the ground test.

## 5. Inflight background and sensitivity

One of the important goals of the balloon flights was to measure the background for the CZT detector in order to determine the InFOC $\mu\text{S}$  sensitivity and to demonstrate the suitability of our active CsI shield. Figure 10 shows the InFOC $\mu\text{S}$  detector background obtained in the 2004 flight. The measured background from a 5.2-hour observation is rather flat from 20–150 keV. This background spectrum was obtained by the following analysis. During our observation, the pointing direction fluctuated by a few arcmin. First we reconstructed an X-ray image of a target according to the pointing information based on attitude sensors, such as a rate gyro and star camera onboard. A point source image was clearly seen in the reconstructed

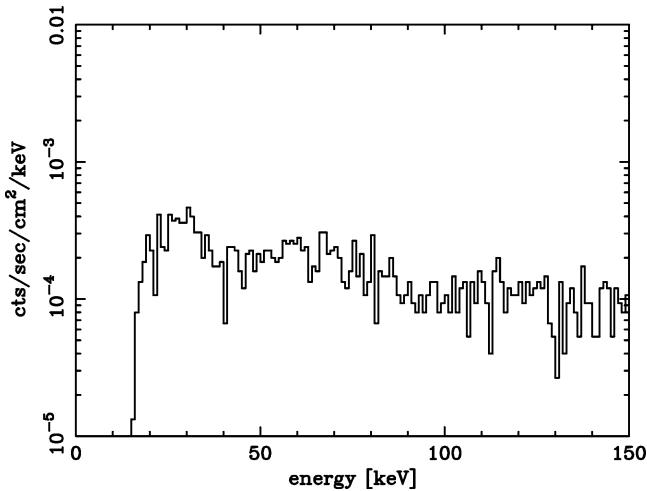
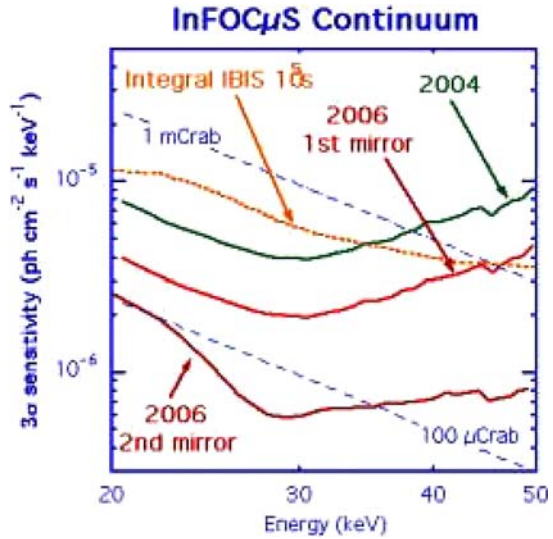


**Fig. 10** Detector background spectrum measured during the Sep. 2004 flight at altitude of 35.2 km (residual atmosphere =  $5.4 \text{ g cm}^{-2}$ ). Events vetoed by the anticoincidence shield have been removed.

X-ray image (Ogasaka et al., 2005). We were able to eliminate events from a source region, which is a circle centered at the image peak with a 5-arcmin radius. We take events outside the source region as background events. And noisy pixels are also masked so that we used only active pixels as the detector area. Note that according to the mirror PSF, the background events still may contain events from the target for about 8% of the source photons at largest. Finally the average background in 20–50 keV was obtained to be  $2.9 \times 10^{-4} \text{ cts cm}^{-2} \text{ sec}^{-1} \text{ keV}^{-1}$ . We also find that 97.3% of the background is rejected by the active CsI shield as vetoed events (Okajima et al., 2005). Passive shielding alone cannot reduce the background rate as it will be dominated by local particle interactions. This background is dominated by internal beta-decay as is usual for heavily shielded detectors. Our background is the lowest background ever achieved in balloon flights. This measurement was taken at the float altitude of 35.2 km ( $5.4 \text{ g cm}^{-2}$ ) without using any depth determination techniques to further reduce the background. This result is consistent with that in the previous InFOC $\mu$ S flights (Baumgartner et al., 2003).

According to the measured background and effective area of the mirror, we can estimate the InFOC $\mu$ S sensitivity as shown in Figure 11. We achieved the sensitivity as low as  $5 \times 10^{-6} \text{ cts cm}^{-2} \text{ sec}^{-1} \text{ keV}^{-1}$  with 8-hour observations (in 20–50 keV and three sigma detection). This is more than one order of magnitude lower than that of non focusing instruments onboard previous experiments, such as *HEAO* and *Ginga*. And the *INTEGRAL* sensitivity ( $10^5 \text{ sec}$  exposure) is comparable with the InFOC $\mu$ S sensitivity with only 8-hour exposure, which is a typical long exposure for one target in balloon experiments. We plan a further improvement to achieve the sensitivity of better than the 100  $\mu$ Crab level. The new hard X-ray mirror will have an angular resolution of 1 arcmin and effective area improved by 50%. This would be a factor of four improvement in the sensitivity. And also we will have two newly developed focal plane detector and shield units for both of the mirrors. The detectors have 1.5 mm pixels and a thinner CZT of 0.5 mm. This would be another factor of two improvement in the sensitivity. In total we would improve factor of 8 as shown in Figure 10.

**Fig. 11** InFOC $\mu$ S sensitivity plot. 2004 curve is as-flown. 2006 curves are also shown. The sensitivity is for an 8-hour observation,  $\Delta E/E = 2$ , typical elevation profile and atmospheric absorption. The IBIS curve is from the AO-2 observers manual, but IBIS is systematics-limited at this level.



## 6. Summary

The InFOC $\mu$ S hard X-ray imaging telescope was successfully flown on September 16–17, 2004, from Fort Sumner, NM. The telescope consists of the depth-graded Pt/C multilayer hard X-ray mirror and CdZnTe pixellated detector. Its effective area is 49 cm<sup>2</sup> at 30 keV, angular resolution 2.4 arcmin (HPD), and field of view 11 arcmin (FWHM). The focal plane detector has the 12 × 12 segmented array of 2 mm square detector pixels. The averaged energy resolution is 4.4 keV at 60 keV. The detector is also surrounded by a 3-cm thick CsI anti coincidence shield to reduce background from particles and photons not incident along the mirror focal direction. The in-flight background is  $2.9 \times 10^{-4}$  cts cm<sup>-2</sup> sec<sup>-1</sup> keV<sup>-1</sup> in the 20–50 keV band, which is the lowest background in balloon experiments owing to the small detector volume and the active shield. Based on the in-flight background, InFOC $\mu$ S achieved the sensitivity as low as  $5 \times 10^{-6}$  cts cm<sup>-2</sup> sec<sup>-1</sup> keV<sup>-1</sup> with 8-hour observations (in 20–50 keV and three sigma detection). We plan to fly with the improvements on the mirror and detector. And we will be archiving 8 times greater sensitivity and exploring the hard X-ray universe.

## References

- Baumgartner, W., et al.: Proc of SPIE **4851**, 945 (2003)
- Kunieda, H., et al.: Applied Optics **40**, 553 (2001)
- Ogasaka, Y., et al.: Proc of SPIE **5900**, 217 (2005)
- Okajima, T., et al.: Proc of SPIE **5898**, 452 (2005)
- Shibata, R., et al.: Proc of SPIE **5900**, 205 (2005)